AMERICAN ACADEMY OF OPHTHALMOLOGY®

Posterior Eye Shape in Myopia

Jost B. Jonas, MD,[1,2,3,4,5,*] *Songhomitra Panda-Jonas, MD,*[1,3,6,*] *Zhe Pan, MD,*[7] *Jie Xu, MD,*[7] *Ya Xing Wang, MD*[7]

Purpose: To explore prevalence and associated factors of abnormalities of the posterior eye shape in dependence of axial length.

Design: Population-based study.

Participants: Of the participants (n = 3468) of the Beijing Eye Study, we included all eyes with an axial length of ≥25 mm, and a randomized sample of eyes with an axial length of <25 mm.

Methods: Using 30°-wide, serial horizontal, and fovea-centered radial, OCT images, we examined location and depth of the most posterior point of the retinal pigment epithelium/Bruch's membrane line (PP-RPE/BML).

Main Outcome Measures: Prevalence and depth of an extrafoveal PP-RPE/BML.

Results: The study included 366 eyes (314 individuals). On the radial OCT scans, the PP-RPE/BML was located in the foveola in 190 (51.9%) eyes, in 121 (33.1%) eyes in the 6 o'clock part of the vertical meridian (distance to foveola: 1.73 ± 0.70 mm), and in 54 (14.8%) eyes in the 12 o'clock part of the vertical meridian (fovea distance: 2.01 ± 0.66 mm). On the horizontal OCT scans, the PP-RPE/BML was located in the foveola in 304 (83.1%) eyes, between foveola and optic disc in 36 (9.8%) eyes (fovea distance: 1.59 ± 0.76 mm), and temporal to the foveola in 26 (7.1%) eyes (fovea distance: 1.20 ± 0.60 mm). Higher prevalence of an extrafoveal PP-RPE/BML correlated with longer axial length (odds ratio [OR]: 1.55; 95% confidence interval [CI]: 1.28, 1.89), higher corneal astigmatism (OR: 1.78; 95% CI: 1.14, 2.79), and female sex (OR: 2.74; 95% CI: 1.30, 5.77). The curvature of the RPE/BML at the posterior pole was similar to the RPE/BML curvature outside of the posterior pole in 309 (84.4%) eyes, and it was steeper (i.e., smaller curvature radius) in 57 (15.6%) eyes. In these eyes, axial length was longer (24.41 ± 1.78 mm versus 27.74 ± 1.88 mm; $P < 0.001$).

Conclusions: With longer axial length, the foveola is more often located outside of the geometrical posterior pole. It may be of importance for biometric axial length measurements. An extrafoveal location of the PP-RPE/BML may be due to an axial elongation-associated, meridionally asymmetric enlargement of Bruch's membrane in the fundus midperiphery.

Financial Disclosure(s): Proprietary or commercial disclosure may be found in the Footnotes and Disclosures at the end of this article. *Ophthalmology Science 2024;4:100575* © *2024 by the American Academy of Ophthalmology. This is an open access article under the CC BY-NC-ND license (http://creativecommons.org/licenses/by-nc-nd/4.0/).*

During ocular development, the eye shape changes from an oblate ellipsoid or sphere in a newborn to an ellipsoid prolate in an axially myopic adult.[1,2] Applying sonography, magnetic resonance imaging (MRI), and histomorphometry, studies have revealed that this process of axial myopization is associated predominantly with an increase in the sagittal diameter of the eye, whereas the horizontal and vertical globe diameters increase by <0.2 mm for each millimeter of axial elongation beyond a total axial length of 24 mm.[3–11] One may assume that the foveola forming the end of the optical axis is located, and remains to be located during the process of axial elongation, at the most posterior part of the posterior retina. Most of the previous studies applying nuclear MRI assessed the ocular shape based on the outer scleral surface, but they could not precisely determine the location of the foveola. Only in the study performed by Hoang et al,[12] a newly developed MRI algorithm was applied to locate the foveola in 82 eyes. Because of the scarcity of information about the position of the foveola in relationship to the posterior globe of the eye, we performed this investigation using OCT imaging to explore the location of the foveola and its spatial relationship to the most posterior location of the posterior fundus in dependence on axial length and other ocular and systemic parameters. We defined foveola as the region at which the retina consisted only of photoreceptors and which showed the characteristic depression in the retinal contour. The posterior pole was geometrically defined as the location at which the retinal pigment epithelium/Bruch's membrane line (PP-RPE/BML) was located most posteriorly on the OCT scan running horizontally through the foveola. To obtain data representative of the general population, we recruited the study participants in a population-based manner.

Methods

The Beijing Eye Study is a population-based investigation that was performed in an urban region of Central Beijing and in a rural area

https://doi.org/10.1016/j.xops.2024.100575
ISSN 2666-9145/24

on the outskirts of Beijing.[13,14] The investigation was approved by The Medical Ethics Committee of the Beijing Tongren Hospital, with all study participants giving their written informed consent for being included in the study. All research adhered to the tenets of the Declaration of Helsinki. Eligible for participation were all individuals who lived in the study regions and had an age of ≥50 years. Of 4403 eligible individuals, the Beijing Eye Study was composed of 3468 (78.8%) subjects with a mean age of 64.6 ± 9.8 years (range: 50−93 years).[13,14] Of this total population of the Beijing Eye Study, we included in the present investigation all eyes with a myopic refractive error of ≥−8 diopters, all eyes with an axial length ≥25.0 mm, and a randomized sample of eyes with an axial length of <25 mm. We defined moderate myopia by an axial length of ≥24.50 mm and <26.5 mm, and high myopia by an axial length of ≥26.5 mm. Eyes with an epiretinal membrane affecting the foveola and which might have caused a tractional displacement of the foveola were excluded.

The list of examinations performed included automatic refractometry and measurement of best-corrected visual acuity, photography of the optic disc and macula (CR6-45NM Camera; Canon), optical low-coherence reflectometry (Lenstar 900 Optical Biometer; Haag-Streit) for measurement of axial length (performed in right eyes only), noncontact tonometry (CT-60 computerized tonometer; Topcon), and spectral-domain OCT (Spectralis OCT; Heidelberg Engineering). The macular region was scanned by a cube scan mode with 31 continuous horizontal B scans each consisting of 100 averaged scans. Covering an area of 30° × 25°, the examined macular region was centered on the foveola. The image penetration resolution was 3.87 µm/pixel (z-resolution). In addition, we took 6 scans which were centered on the foveola and were arranged in a star-like manner.

By examining all horizontal macular OCT scans and the radial OCT star scans of the macula, we assessed the following:

1. The most posterior point (PP) of the PP-RPE/BML was examined on all scans running through the foveola. If the RPE/BML ran straight from the foveola to the temporal optic disc border without a localized deepening, a PP-RPE/BML was not present (Figs 1−5). If the PP-RPE/BML was not located in the foveola, its distance to the foveola and its depth of the PP-RPE/BML relative to the foveola reference was measured in the sagittal direction. In eyes with a dome-shaped configuration of the macula, the RPE/BML at the base of both sides of the dome-shaped configuration of the macula was linked, and this artificial line was taken to assess the PP-RPE/BML. In a similar manner, in eyes with a macular ridge, the RPE/BML at the base of both sides of the ridge was linked, and this artificial line was taken to assess the PP-RPE/BML.
2. The difference in sagittal position of the RPE/BML in the foveola and of the RPE/BML at the temporal optic disc border; and
3. Whether the curvature radius of the RPE/BML was smaller (i.e., more curved) at the posterior pole (defined as the most posterior location of the RPE/BML) than outside of the posterior pole (Fig 4).

Care was taken that the OCT images were sharply focused along the entire length of the scan and that the images were centered on the foveola, to avoid an artifact due to an artificially oblique image taking. An inclusion criterion was that the foveola had to be located in a central image part extending over less than one-fifth of the width of the entire image.

Using a statistical software package (SPSS for Windows, version 28.0, IBM-SPSS), we determined the mean values and their 95% confidence intervals (CIs) of prevalence-related parameters, and the mean values and their standard deviations of continuous parameters. We assessed the relationships between the variables first in univariate analyses, followed by multivariable analyses. The multivariable analyses consisted of the main outcome parameter as the dependent parameter, and independent variables were all those parameters that were correlated ($P < 0.10$) with the outcome parameter in the univariate analysis. Out of the list of independent variables, we then dropped in a step-by-step manner all those factors that were no longer significantly associated with the dependent variable. For binary parameters (e.g., prevalence of posterior fundus irregularities), we applied binary regression analyses, and we used linear regression analyses in the case of continuous parameters. We assessed the odds ratios and their 95% CIs in the binary regression analyses, and we determined the nonstandardized regression coefficient B and its 95% CIs and the standardized regression coefficient β in the case of linear regression analyses. A 2-sided P value of <0.05 was regarded to be statistically significant.

Results

The study cohort consisted of 366 eyes from 314 individuals (161 men, 51.3%). Participants had a mean age of 63.7 ± 9.7 years (median: 62.0 years; range: 50−93 years) and a mean axial length of 25.2 ± 2.1 mm (median: 25.2 mm; range: 20.16−31.50 mm). The study cohort and the group of the excluded participants of the Beijing Eye Study did not differ in age (63.7 ± 9.7 years versus 64.7 ± 9.8 years; $P = 0.07$), although the study cohort contained a higher percentage of men (50.5% versus 43.0%; $P = 0.005$). The study cohort included 127 nonmyopic eyes, 153 moderately myopic eyes, and 86 highly myopic eyes (Table 1).

On the radial OCT scans, the PP-RPE/BML was located in the foveola in 190 (51.9%) eyes, in 121 (33.1%) eyes in the 6 o'clock part of the vertical meridian, in 54 (14.8%) eyes in the 12 o'clock part of the vertical meridian, and in 1 (0.3%) eye in the 4 o'clock position of the meridian running from 4 o'clock to 10 o'clock (Table 2). The distance from the foveola to extrafoveally located PP-RPE/BMLs was 1.73 ± 0.70 mm in the eyes located in the 6 o'clock meridian, 2.01 ± 0.66 mm in the eyes located in the 12 o'clock position, and 1.55 mm in the eye located in the 4 o'clock meridian (Table 2).

A higher prevalence of an extrafoveal location of the PP-RPE/BMLs on the radial OCT scans was associated with longer axial length (odds ratio: 1.27; 95% CI: 1.12, 1.43; $P < 0.001$), whereas it was not correlated with age ($P = 0.58$), sex ($P = 0.47$), mean anterior corneal curvature radius ($P = 0.29$), corneal astigmatism ($P = 0.29$), and intraocular pressure ($P = 0.79$). The depth of an extrafoveal PP-RPE/BML correlated (univariate analysis) with longer axial length ($P < 0.001$), female sex ($P < 0.001$), and higher corneal astigmatism ($P = 0.005$), and it was statistically independent of age ($P = 0.07$), intraocular pressure ($P = 0.79$) and anterior corneal curvature radius ($P = 0.53$). In multivariable analysis, a deeper depth of an extrafoveal PP-RPE/BML increased with longer axial length ($P < 0.001$), female gender ($P = 0.002$), and higher corneal astigmatism ($P = 0.03$) (Table 3).

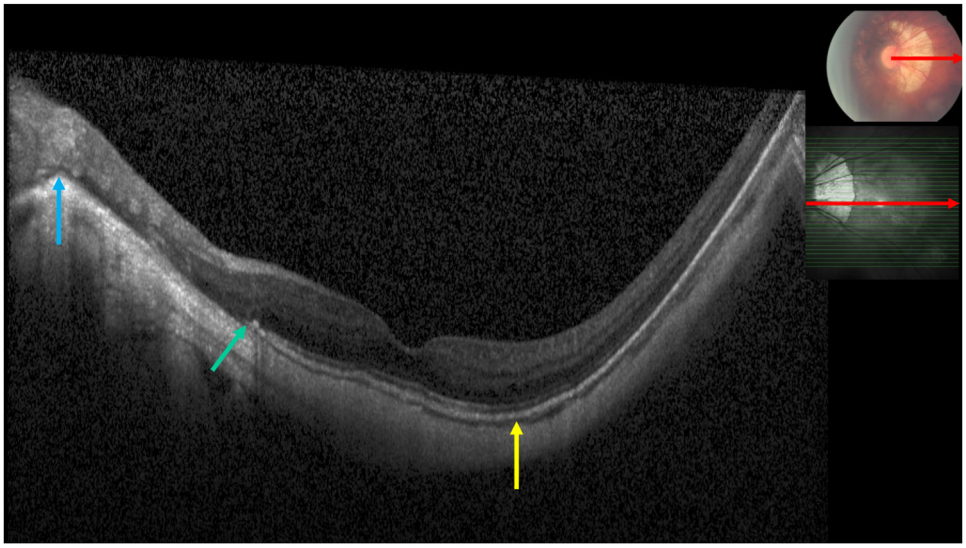

Figure 1. OCT scan drawn horizontally through the fovea, with the most posterior part of the retinal pigment epithelium/Bruch's membrane line (RPE/BML) (yellow arrow) located temporal to the fovea, and with the inner scleral surface line (in continuation of the RPE/BML) at the temporal optic disc border (blue arrow) located more anteriorly than the RPE/BML in the fovea; green arrow: end of Bruch's membrane, i.e., peripheral border of parapapillary γ zone. Red arrow: location and orientation of the scan.

Upon examination of the horizontal OCT scans running through the foveola, the PP-RPE/BML was found in the foveola for 304 eyes (83.1%), located nasally to the fovea in 36 eyes (9.8%), while located temporal to the foveola in 26 eyes (7.1%) (Table 2). The distance from the foveola to extrafoveally located PP-RPE/BMLs is presented in Table 2.

In multivariable binary regression analysis, a higher prevalence of an extrafoveal location of the PP-RPE/BML on the horizontal OCT scan was significantly associated with longer axial length ($P < 0.001$), higher corneal astigmatism ($P = 0.01$) and female sex ($P = 0.008$), whereas it was not correlated with age ($P = 0.10$), mean anterior corneal curvature radius ($P = 0.90$), and intraocular pressure ($P = 0.82$) (Table 3). A deeper depth of an extrafoveally located PP-RPE/BML in relationship to the height of the line in the foveola was associated with longer axial length ($P = 0.001$), female sex ($P = 0.01$), older age ($P = 0.02$), and higher corneal astigmatism ($P = 0.001$). In multivariable linear regression analysis, a deeper depth of an extrafoveally located PP-RPE/BML in relationship to the

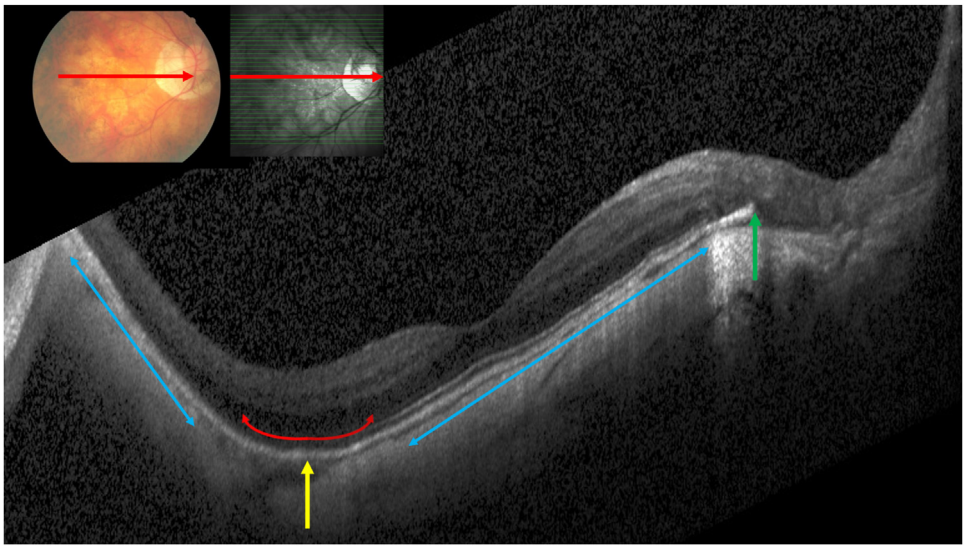

Figure 2. OCT scan drawn horizontally through the fovea, with the most posterior part of the retinal pigment epithelium/Bruch's membrane line (RPE/BML) (yellow arrow) located temporal to the fovea, and with the end of the RPE/BML at the temporal optic disc border (green arrow) located more anteriorly than the RPE/BML in the fovea. Note: difference in the curvature radius between the RPE/BML at the posterior pole (red, double-arrowed line) and in the region outside of the posterior pole (blue double-arrowed line). Red arrow: location and orientation of the scan.

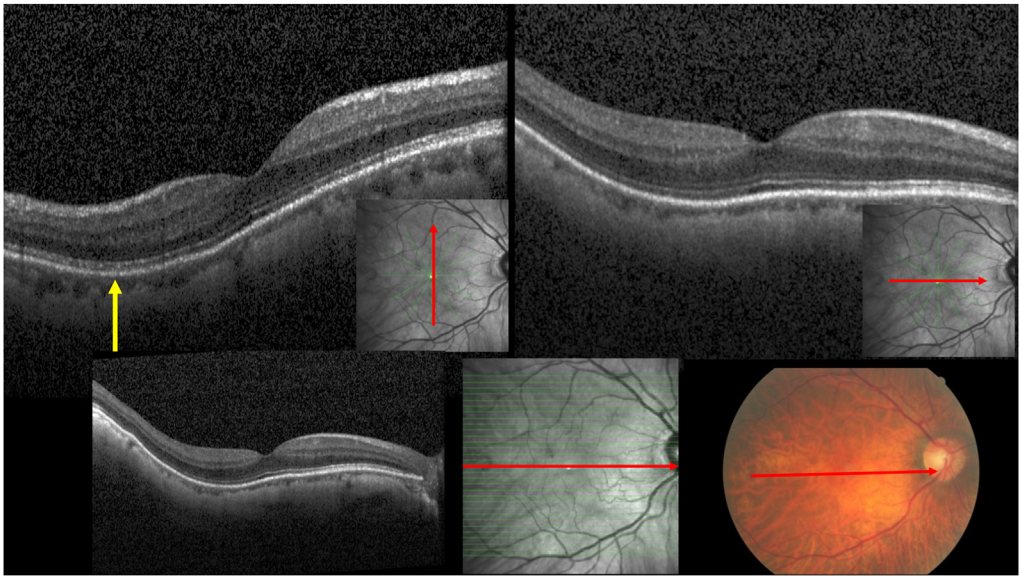

Figure 3. OCT scans drawn vertically and horizontally through the fovea. Note: On the vertical scan, the most posterior part of the retinal pigment epithelium/Bruch's membrane line (RPE/BML) is located posterior to the fovea (yellow arrow), whereas the horizontal scan shows a RPE/BML without major heights or depths. Red arrows: location and orientation of the scan.

height of the line in the foveola correlated with longer axial length ($P = 0.003$) and a higher corneal astigmatism ($P = 0.001$) (Table 3).

Axial length increased significantly ($P < 0.001$) with the location of the PP-RPE/BML, from an intrafoveal PP-RPE/BML location (axial length: 24.50 ± 1.90 mm) to a PP-RPE/BML location nasal to the fovea (26.03 ± 1.92 mm) and finally to a PP-RPE/BML location temporal to the fovea (26.95 ± 2.80 mm) (Fig 6). Correspondingly, the PP-RPE/BML on the horizontal OCT scans through the fovea was located outside of the foveola in 4.1% (95% CI: 0.6, 7.6) of the eyes of the nonmyopic group, 15.0% (95% CI: 9.0, 21.0) of the eyes of the moderately myopic group, and 35.4% (95% CI: 21.4, 49.4) of the eyes of the highly myopic group.

A dome-shaped configuration of the fovea was detected in 7 eyes (7/366 or 1.9%). In 3 of these 7 eyes, the PP-RPE/BML was located extrafoveally, whereas in the remaining 4 eyes, the foveola, including its dome-shaped configuration, was located at the posterior pole.

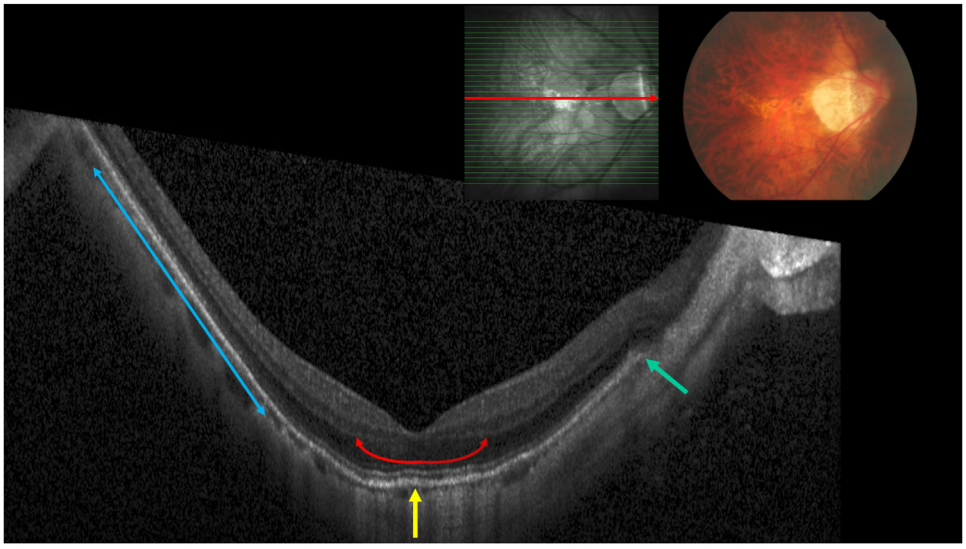

Figure 4. OCT scan drawn horizontally through the fovea, with a difference in the curvature radius between the retinal pigment epithelium/Bruch's membrane line (RPE/BML) at the posterior pole (red, double-arrowed line) and in the region outside of the posterior pole (blue double-arrowed line); yellow arrow: position of the foveola at the most posterior point of the RPE/BML; green arrow: end of Bruch's membrane, i.e., peripheral border of parapapillary γ zone; red arrow: location and orientation of the scan.

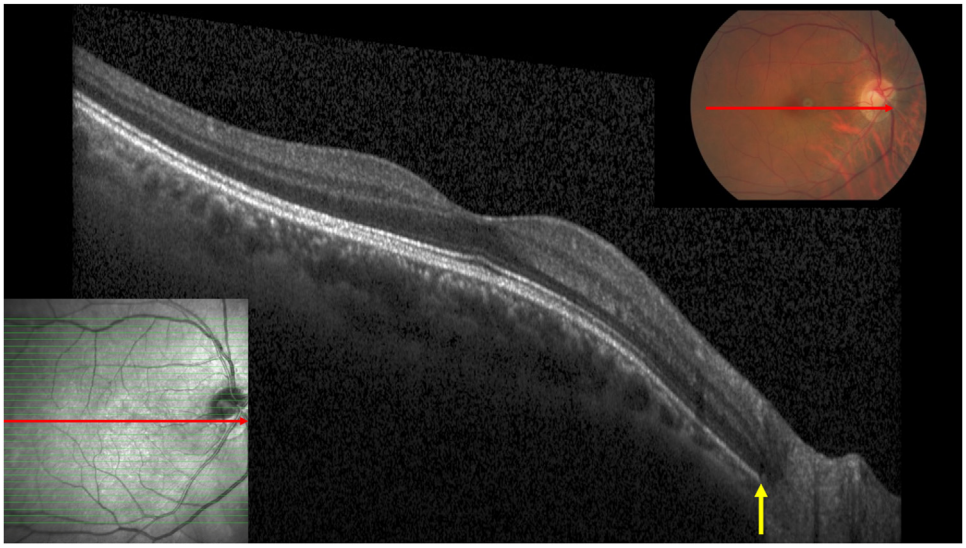

Figure 5. OCT scan drawn horizontally through the fovea, with the most posterior part of the retinal pigment epithelium/Bruch's membrane line located at the temporal optic disc border (yellow arrow). Red arrow: location and orientation of the scan.

The curvature of the RPE/BML at the posterior pole was identical to the curvature of the RPE/BML outside of the posterior pole in 309 (84.4%; 95% CI: 80.7, 88.2) eyes, and it was steeper (i.e., a smaller curvature radius) in 57 (15.6%; 95% CI: 12.1, 19.1) of the eyes. Axial length was significantly longer in the eyes with a difference in the RPE/BML curvature than in the eyes without such a difference (24.41 ± 1.78 mm versus 27.74 ± 1.88 mm; $P < 0.001$) (Fig 7). In univariate analysis, the prevalence of a discrepancy between a steeper posterior pole curvature and a flatter curvature outside of the posterior pole increased with longer axial length ($P < 0.001$), higher corneal astigmatism ($P = 0.003$), older age ($P < 0.001$) and female sex ($P < 0.001$). In multivariable analysis, a higher prevalence remained to be significantly associated with longer axial length ($P < 0.001$), female sex ($P = 0.002$), and older age ($P = 0.01$), whereas corneal astigmatism was no longer significantly associated ($P = 0.90$) (Table 2).

In 148 (40.4%; 95% CI: 35.4, 45.4) eyes, the most posteriorly located site of the RPE/BML at the posterior fundus was at the temporal optic disc border without an additional deepening between the optic nerve head and the foveola (Fig 5). A higher prevalence of such a configuration was correlated with higher anterior corneal curvature radius ($P = 0.02$), whereas it was not significantly associated with axial length ($P = 0.26$), corneal astigmatism ($P = 0.55$), age ($P = 0.17$) and sex ($P = 0.08$). In multivariable analysis, none of the associations remained to be statistically significant. Including all eyes of the study cohort or including only eyes with such a configuration, the difference in the sagittal depth between the RPE/BML at the fovea and the RPE/BML at the temporal optic disc border was 0.85 ± 0.178 µm (median: 0 µm, range: 0.00−1.15 µm) and 211 ± 228 µm (median: 100 µm; range: 25−1.15 µm), respectively. It was significantly associated with longer axial length ($P < 0.001$; β: 0.32; B: 0.13; 95% CI: 0.09, 0.29), whereas it did not correlate with anterior corneal curvature radius ($P = 0.35$), corneal astigmatism ($P = 0.57$), age ($P = 0.09$), and sex ($P = 0.18$).

In 81 (22.1%; 95% CI: 18.1, 26.1) eyes, the end of the RPE/BML at the temporal optic disc border was located more anteriorly than the PP-RPE/BML (Figs 1, 2, 4). A higher prevalence of such a configuration correlated with longer axial length ($P < 0.001$), higher corneal astigmatism ($P = 0.03$), and older age ($P = 0.02$); it was not significantly associated with anterior corneal curvature radius ($P = 0.96$) and sex ($P = 0.21$). In multivariable analysis, it remained to be significantly correlated only with longer axial length ($P < 0.001$; odds ratio: 1.19; 95% CI: 0.75, 1.83). Taking all eyes of the study population (with all eyes without elevation taken as 0 values) or only eyes with such a configuration, the height of the RPE/BML at the temporal optic disc border above the foveal level was 140 ± 332 (median: 0 µm; range: 0.00−1725 µm) and 632 ± 434 µm (median: 550 µm; range: 50−1725 µm), respectively. In univariate analysis, the amount of elevation correlated significantly with longer axial length ($P < 0.001$), higher amount of corneal astigmatism ($P = 0.02$), older age ($P = 0.01$), and

Table 1. Demographic Data of the Study Population Stratified by the Degree of Myopia

	Nonmyopic eyes	Moderately Myopic Eyes	Highly Myopic Eyes
Number of eyes	127	153	86
Age (yrs)	60.3 ± 8.9	66.4 ± 9.5	64.0 ± 9.0
Men/women	54 (42.5%)/73 (57.5%)	96 (62.7%)/57 (37.3%)	35 (40.7%)/51 (59.3%)

Table 2. Prevalence and Location of the Most PP on the RPE/BML in the Beijing Eye Study

Location of PP-RPE/BML	n	Prevalence	95% CI (%)	Distance from the Fovea to PP-RPE/BML (mm)	Depth of PP-RPE/BML (μm)
Evaluation in OCT radial scans centered at the fovea					
In the fovea	190	51.9%	46.9, 56.9	–	–
In extrafoveal locations					
In the 12 o'clock part of the vertical meridian	54	14.8%	11.1, 18.4	2.01 ± 0.66	96 ± 56
In the 6 o'clock part of the vertical meridian	121	33.1%	28.1, 38.1	1.73 ± 0.70	152 ± 146
In the 4 o'clock position of the meridian running from 4 o'clock to 10 o'clock	1	0.30%	0.0, 1.0	1.55	124
Evaluation in horizontal OCT scan					
In the fovea	304	83.1%	79.2, 86.9	–	–
In extrafoveal locations					
Nasal to the fovea	36	9.8%	6.8, 12.9	1.59 ± 0.76	119 ± 142
Temporal to the fovea	26	7.1%	4.5, 9.8	1.20 ± 0.60	71 ± 46

BML = Bruch's membrane line; CI = confidence interval; PP = posterior point; RPE = retinal pigment epithelium.

female sex ($P = 0.03$); it was not significantly associated with the anterior corneal curvature radius ($P = 0.96$). In multivariable linear regression analysis, the height of the RPE/BML at the temporal optic disc border as compared with the foveal level correlated with longer axial length ($P < 0.001$) and female sex ($P = 0.006$) (Table 2).

Discussion

In our study cohort, the prevalence of a location of the foveola outside of the posterior pole and the distance between the foveola and the posterior pole increased with longer axial length. In a parallel manner, a higher prevalence

Table 3. Associations (Multivariable) of Prevalence or Depth of the Most PP on the RPE/BML, if Located Extrafoveally, in the Beijing Eye Study

Depth of an extrafoveally located PP-RPE/BML on radial OCT scans in relationship to the foveola					
Parameter	*Standardized Regression Coefficient β*	*Nonstandardized Regression Coefficient B*	*95% CIs of B*	*P Value*	*VIF*
Axial length (mm)	0.28	12.3	7.5, 17.1	<0.001	1.02
Male/female sex	0.17	30.2	10.7, 49.6	0.002	1.02
Cornea astigmatism (diopters)	0.12	13.9	1.50, 26.3	0.03	1.01
Prevalence of an extrafoveal location of the PP-RPE/BML on the horizontal OCT scan					
	OR	95% CI of OR	*P* Value		
Axial length (mm)	1.55	1.28, 1.89	<0.001	–	–
Male/female sex	2.74	1.30, 5.77	0.008	–	–
Corneal astigmatism (diopters)	1.78	1.14, 2.79	0.01	–	–
Depth of an extrafoveally located deepest point of the RPE/BML on the horizontal OCT scan					
	β	B	95% CI of B	*P* Value	VIF
Axial length (mm)	0.17	4.39	1.49, 7.29	0.003	1.01
Corneal astigmatism (diopters)	0.19	12.7	5.13, 20.2	0.001	1.01
Prevalence of a discrepancy between a steeper curvature at the posterior pole and a flatter curvature outside of the posterior pole					
	OR	95% CI of OR	*P* Value		
Axial length (mm)	3.72	2.38, 5.81	<0.001	–	–
Male/female sex	5.55	1.85, 16.7	0.002	–	–
Age (yrs)	1.07	1.01, 1.14	0.01	–	–
Height of the RPE/BML at the temporal optic disc border as compared with the foveal level					
	β	B	95% CIs of B	*P* Value	VIF
Axial length (mm)	0.40	50.1	37.1, 63.0	<0.001	1.01
Male/female sex	0.15	74.6	21.4, 128	0.006	1.01

BML = Bruch's membrane line; CI = confidence interval; OR = odds ratio; PP = posterior point; RPE = retinal pigment epithelium; VIF = variance inflation factor.

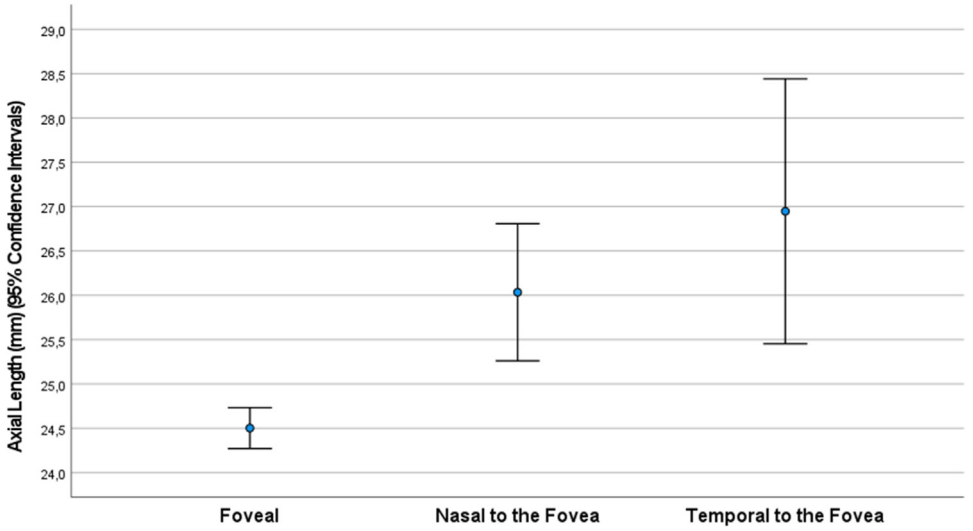

Figure 6. Graph showing the distribution of axial length stratified by the location of the most posterior point of the retinal pigment epithelium/Bruch's membrane line on the horizontal OCT scan running through the fovea in the Beijing Eye Study.

of a more curved contour line at the posterior pole as compared with the region just outside of the posterior pole increased with longer axial length and older age.

In previous studies, the contour of the posterior ocular segment has already been examined. Examining the influence of normal eye movements results on gaze-induced globe deformations in highly myopic eyes with posterior scleral staphylomas, Hoang et al[12] obtained 3-dimensional MRI scans with the study participants looking into 5 directions. They detected deformations of the posterior globe shape in dependence on the gaze direction, in particular a reversible, instantaneous increase in vitreous cavity axial volume in downgaze. Similar results were obtained if the eye shape under different gaze conditions were examined by sonography.[15]

The observation that the foveola was located anteriorly to the posterior pole in some eyes is of clinical importance for biometric measurement of the sagittal ocular length as the basis of the determination of the refractive power of intraocular lenses to be implanted during cataract surgery. Using an extrafoveal PP-RPE/BML as the end of the optical axis could lead to an underestimation of the necessary refractive power of the intraocular lens.[16–18] Accordingly, previous studies have revealed that hyperopic refractive outcomes of cataract surgery can occur in highly myopic patients even if third-generation intraocular lens formulas were applied,

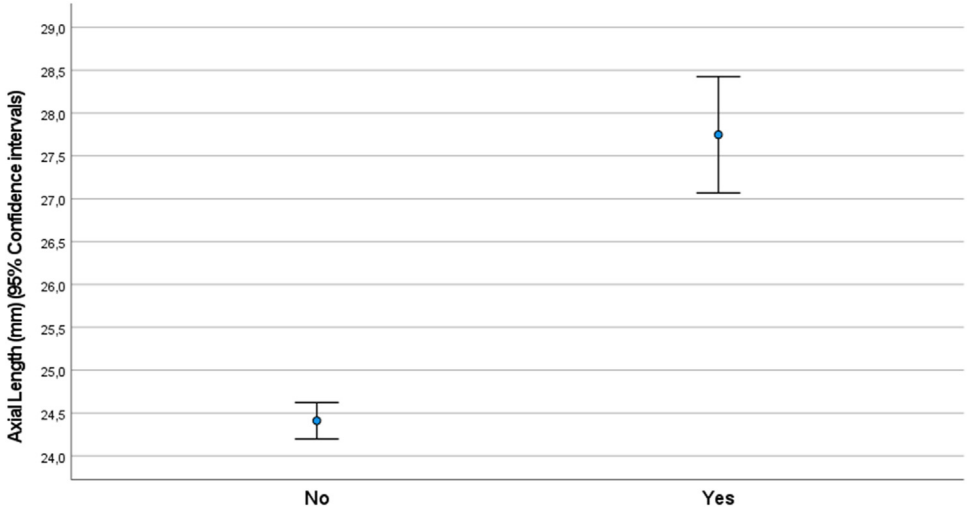

Figure 7. Graph showing the distribution of axial length stratified by the occurrence of a difference in the curvature of the retinal pigment epithelium/Bruch's membrane line between the foveal region and the extrafoveal region in the Beijing Eye Study.

though without adjustments.[16] Future studies may address whether the assessment of an extrafoveal location of the PP-RPE/BML in myopic eyes and taking it into consideration for the calculation of the intraocular lens in cataract surgery may be helpful to improve the prediction of the postoperative refractive error. Future investigations may also explore the relationship between an extrafoveal location of the PP-RPE/BML and the occurrence of pseudostrabismus.

The finding that with increasing axial length the prevalence of an extrafoveal PP-RPE/BML increased may be taken as a hint that it is not the foveola that governs the process of axial elongation in the process of emmetropization. According to a recently formulated hypothesis, myopic axial elongation may occur through a retina-induced growth and enlargement of Bruch's membrane (BM) in the fundus midperiphery.[2,19] Such a mechanism could explain several myopia-associated morphologic features of the fundus. It includes the development of parapapillary γ zone in moderately myopic eyes through a shift of BM opening of the optic nerve head canal into the foveal direction, also associated with a vertical ovalization of the optic disc shape due to a shortening of the ophthalmoscopically visible horizontal disc diameter, and associated with a fovea−optic disc distance elongation, a reduction in angle κ between the temporal vascular arcades, and a straightening/stretching of the papillo-macular retinal blood vessels and retinal nerve fibers. The notion of axial elongation-associated growth of BM in the fundus midperiphery is also in agreement with a thinning of the retina and reduction in the density of RPE cells and photoreceptors in the fundus midperiphery, whereas retinal thickness and RPE cell density in the macula are mostly independent of axial length and with the thinning of the choroid most marked at the posterior pole. The location of the presumed BM growth in the fundus midperiphery coincides with the presumed location of the sensory arm of the intraocular feedback mechanism governing myopic axial elongation. In the recently developed therapy using centric-peripheral overcorrecting contact lenses and glasses to reduce axial myopia progression in children and adolescents, the targeted fundus location is the midperiphery.[20] It agrees with the location of the presumed efferent arm of the feedback mechanism, i.e., BM enlargement, in the fundus midperiphery.

If the growth of BM in the fundus midperiphery is the mechanism of myopic axial elongation, and if this BM enlargement is not equal in all meridians but, to cite an example, is larger in temporal meridian than in the nasal meridian, the most posterior part of the RPE/BML would get located temporal to the foveola. If in the reverse manner, BM enlargement is larger in the nasal versus temporal meridian, the most posterior location of the RPE/BML would be located between the fovea and the optic disc, or the RPE/BML declines toward the temporal optic disc border in a straight manner (Fig 5). In a similar manner, if the inferior versus superior meridian shows a more marked BM growth, the most posterior location of the RPE/BML would be located inferior to the fovea in the vertical OCT scan running through the fovea. The findings made in the present study may thus be explainable by an asymmetrical enlargement of BM in the fundus midperiphery, with the meridian having the most marked BM growth and also having the most posterior position of the RPE/BML (Fig 8). In agreement with the notion of a dependence of the foveal versus the extrafoveal location of the PP-RPE/BML on an asymmetry between 2 perpendicular planes are previous reports on intermeridional differences in scleral thinning and presumable scleral elongation in eyes with axial elongation.[21] Dhakal et al[21] found that the inferior anterior scleral thickness decreased with a higher degree of myopia, whereas there were no differences in anterior scleral thickness between the temporal meridian and nasal meridian.

As an alternative hypothesis, one may discuss that an extrafoveal location of the PP-RPE/BML was due to the presence of a staphyloma with a non−fovea-centered apex, with the prevalence of staphylomas increasing with longer axial length.[1] In the population of the present study, a parafoveal staphyloma was, however, not detected. Limiting this statement is that wide-angle OCT scans were not available; hence, staphylomas might have been overlooked.

Interestingly, the extrafoveal location of the PP-RPE/BML was associated with increased corneal astigmatism (Table 3). It has remained unclear whether such an association would be useful to compensate for an obliqueness of the projection screen of the ocular optical system, i.e., the fovea. Such a functional association is contradicted by the discrepancy in time points when corneal astigmatism (first years of life) and ocular axial length (first 3 decades of life or even later) are determined.

When the observations made in our study are discussed, the limitations of the investigation have to be taken into account. First, we obtained the data in a horizontal raster-scanned and star-scanned manner; however, we did not localize the PP-RPE/BML in a volumetric manner by creating a distortion-corrected volume rendering of the RPE-BML, for example, with an artificial intelligence-assisted adaptive compensation, as recently described by Girard et al.[22] In addition, the localization of the PP-RPE/BML requires that among the study participants there should be reproducible orientation of the eye in the 3-dimensional space, in particular, because any eccentric fixation could be associated with misleading results. However, any eccentric fixation may occur in random directions; hence, that may increase the inaccuracy and noise of the method, without a major influence on the mean and median values. In addition, the prevalence of an extrafoveal location of the PP-RPE/BML increased with axial length, and the increasingly prolate shape of the posterior ocular segment in myopic and highly myopic eyes would still place the foveola at the PP-RPE/BML if eyes with a foveal location of the PP-RPE/BML show an eccentric fixation of approximately $<10°$. Second, using the 6 star-shaped radial scans of the macula capturing only 12 angles across the 360 degrees centered at the fovea did not cover the entire macular region but only the sections of the star, disregarding the region between the radial scans. In view of the relatively smooth shape of the posterior ocular segment, it may, however, be unlikely that the data missed in the

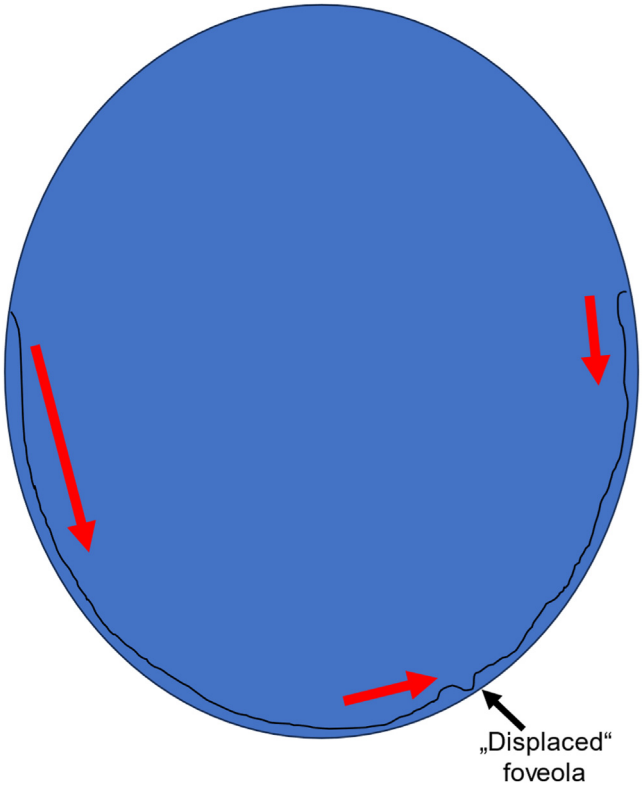

Figure 8. Scheme showing an asymmetry between the temporal meridian and the nasal meridian in a presumed enlargement of Bruch's membrane in the fundus midperiphery, leading a discrepancy between the most posterior part of Bruch's membrane and the foveola.

regions between the macular radial scans might have markedly influenced the results of the study. Again, using a volumetric 3-dimensional reconstruction of the posterior ocular shape might have addressed this limitation in locating the PP-RPE/BML. Third, in line with the 2 factors mentioned above, the orientation of the OCT image depends on the focusing of the scan so that an asymmetrical focusing can lead to an oblique and a falsely skewed image. When performing the OCT imaging, care was therefore taken that the entire region of interest was sharply imaged, and the foveola was located in a central image part extending over less than one-fifth of the width of the entire image. In addition, such a technical artifact which might have led to a skewed presentation of the entire image could not explain the occurrence of a localized backward bowing of the retinal contour. Also, the probability of skewness of the image may have been the same for the left side of the image as for the right side of the image. Such an artifact might therefore have increased the noise of the measurements, but not the mean location of a retinal site imaged to be located more posteriorly than the foveola. Fourth, a discrepancy between the curvature of the RPE/BML at the posterior pole and the curvature outside of the posterior pole was assessed on the horizontal scans running through the foveola, so that such a discrepancy might have been missed if the smallest curvature of the RPE/BML was located outside of this scan, for example, superior or inferior to the fovea. The data of this parameter therefore refer only to the examination of the horizontal foveal scan. Fifth, because we did not use a wide-angle OCT scan, we could not assess the presence of a posterior staphyloma (defined as a local outpouching of the eye wall) or of multiple staphylomas. In the case of an extrafoveal location of the PP-RPE/BML, we could thus not differentiate between a posterior staphyloma located exactly at the posterior pole and a simple discrepancy between the foveal location and the location of the PP-RPE/BML. Future studies may address the question of which aspects of a staphyloma at the posterior pole differ from a discrepancy between the foveal location and the location of the PP-RPE/BML. Sixth, although the study included all highly myopic eyes, only a randomized group of moderately myopic eyes and nonmyopic eyes were included in the study. The data on the prevalence of a PP-RPE/BML dislocation may therefore be representative of the study subgroups (nonmyopic, moderately myopic, and highly myopic), but not of the entire study population due to the higher weightage of the highly myopic subgroup in the total study population.

In conclusion, with a longer axial length, the fovea is increasingly located outside of the geometrical posterior pole. It may be of importance for biometric axial length measurements, and it may be explained by an axial elongation-associated, meridionally asymmetric enlargement of BM in the fundus midperiphery.

Footnotes and Disclosures

Originally received: March 19, 2024.
Final revision: June 18, 2024.
Accepted: June 28, 2024.
Available online: July 6, 2024. Manuscript no. XOPS-D-24-00090R3.

[1] Rothschild Foundation Hospital, Institut Français de Myopie, Paris, France.

[2] Singapore Eye Research Institute, Singapore National Eye Center, Singapore.

[3] Privatpraxis Prof Jonas und Dr. Panda-Jonas, Heidelberg, Germany.

[4] New York Eye and Ear Infirmary of Mount Sinai, Icahn School of Medicine at Mount Sinai, New York, New York.

[5] Tsinghua Medicine, Tsinghua University, Beijing, China.

[6] Department of Ophthalmology, Medical Faculty Heidelberg, Heidelberg University, Heidelberg, Germany.

[7] Beijing Ophthalmology and Visual Sciences Key Laboratory, Beijing Institute of Ophthalmology, Beijing Tongren Hospital, Capital Medical University, Beijing, China.

*J. B. J. and S. P.-J. contributed equally to this work and share the first authorship.

Disclosure(s):

All authors have completed and submitted the ICMJE disclosures form.

The author(s) have made the following disclosure(s):

J.J.B: Patents planned, issued or pending − European patent EP 3 271 392, JP 2021-119187, and US 2021 0340237 A1: "Agents for use in the therapeutic or prophylactic treatment of myopia or hyperopia."

S.P.-J.: Patents planned, issued or pending − European patent EP 3 271 392, JP 2021-119187, and US 2021 0340237 A1: "Agents for use in the therapeutic or prophylactic treatment of myopia or hyperopia."

The other authors have no proprietary or commercial interest in any materials discussed in this article.

Financial Support: Supported by the Research Development Fund of Beijing Municipal Health Commission (2019-4); National Natural Science Foundation of China (82271086). The funder of this study had no role in study design, data collection, data analysis, data interpretation, or writing of the manuscript.

HUMAN SUBJECTS: Human subjects were included in this study. The investigation was approved by The Medical Ethics Committee of the Beijing Tongren Hospital. All research adhered to the tenets of the Declaration of Helsinki. All participants provided informed consent.

No animal subjects were used in this study.

Author Contributions:

Conception and design: Jonas, Panda-Jonas, Wang

Data collection: Jonas, Panda-Jonas, Pan, Xu, Wang

Analysis and interpretation: Jonas, Panda-Jonas, Pan, Xu, Wang

Obtained funding: Wang

Overall responsibility: Jonas, Panda-Jonas, Pan, Xu, Wang

Abbreviations and Acronyms:
BM = Bruch's membrane; **BML** = Bruch's membrane line; **CI** = confidence interval; **MRI** = magnetic resonance imaging; **PP** = posterior point; **RPE** = retinal pigment epithelium.

Keywords:
Axial elongation, Beijing Eye Study, Dome-shaped macula, High myopia, Macular ridges.

Correspondence:
Ya Xing Wang, MD, Beijing Tongren Hospital, 1 Dongjiaomin Lane, Dongcheng, 100730, Beijing, China. E-mail: yaxingw@gmail.com.

References

1. Morgan IG, Ohno-Matsui K, Saw SM. Myopia. *Lancet*. 2012;379:1739−1748.
2. Jonas JB, Jonas RA, Bikbov MM, et al. Myopia: histology, clinical features, and potential implications for the etiology of axial elongation. *Prog Retin Eye Res*. 2023;96:101156.
3. Heine L. Beiträge zur Anatomie des myopischen Auges. *Arch Augenheilk*. 1899;38:277−290.
4. Meyer-Schwickerath G, Gerke E. Biometric studies of the eyeball and retinal detachment. *Br J Ophthalmol*. 1984;68:29−31.
5. Cheng HM, Singh OS, Kwong KK, et al. Shape of the myopic eye as seen with high-resolution magnetic resonance imaging. *Optom Vis Sci*. 1992;69:698−701.
6. Atchison DA, Jones CE, Schmid KL, et al. Eye shape in emmetropia and myopia. *Invest Ophthalmol Vis Sci*. 2004;45:3380−3386.
7. Logan NS, Gilmartin B, Wildsoet CF, Dunne MCM. Posterior retinal contour in adult human anisomyopia. *Invest Ophthalmol Vis Sci*. 2004;45:2152−2162.
8. Guo X, Xiao O, Chen Y, et al. Three-dimensional eye shape, myopic maculopathy, and visual acuity: the Zhongshan Ophthalmic Center-Brien Holden Vision Institute High Myopia Cohort Study. *Ophthalmology*. 2017;124:679−687.
9. Jonas JB, Ohno-Matsui K, Holbach L, Panda-Jonas S. Association between axial length and horizontal and vertical globe diameters. *Graefes Arch Clin Exp Ophthalmol*. 2017;255:237−242.
10. Matsumura S, Kuo AN, Saw SM. An update of eye shape and myopia. *Eye Contact Lens*. 2019;45:279−285.
11. Kneepkens SCM, Marstal K, Polling JR, et al. Eye size and shape in relation to refractive error in children: a magnetic resonance imaging study. *Invest Ophthalmol Vis Sci*. 2023;64:41.
12. Hoang QV, Chang S, Yu DJG, et al. 3-D assessment of gaze-induced eye shape deformations and downgaze-induced vitreous chamber volume increase in highly myopic eyes with staphyloma. *Br J Ophthalmol*. 2021;105:1149−1154.
13. Yan YN, Wang YX, Yang Y, et al. Ten-year progression of myopic maculopathy: the Beijing Eye Study 2001-2011. *Ophthalmology*. 2018;125:1253−1263.
14. Wang YX, Pan Z, Xue CC, et al. Macular outer nuclear layer, ellipsoid zone and outer photoreceptor segment band thickness, axial length and other determinants. *Sci Rep*. 2023;13:5386.
15. Cheong KX, Lim SY, Dan YS, et al. Ultrasound assessment of gaze-induced posterior eyewall deformation in highly myopic eyes. *Invest Ophthalmol Vis Sci*. 2023;64:38.
16. Chong EW, Mehta JS. High myopia and cataract surgery. *Curr Opin Ophthalmol*. 2016;27:45−50.
17. Abulafia A, Barrett GD, Rotenberg M, et al. Intraocular lens power calculation for eyes with an axial length greater than 26.0 mm: comparison of formulas and methods. *J Cataract Refract Surg*. 2015;41:548−556.

18. Elhusseiny AM, Salim S. Cataract surgery in myopic eyes. *Curr Opin Ophthalmol*. 2023;34:64−70.
19. Jonas JB, Ohno-Matsui K, Jiang WJ, Panda-Jonas S. Bruch membrane and the mechanism of myopization: A new theory. *Retina*. 2017;37:1428−1440.
20. Jonas JB, Ang M, Cho P, et al. IMI prevention of myopia and its progression. *Invest Ophthalmol Vis Sci*. 2021;62:6.
21. Dhakal R, Vupparaboina KK, Verkicharla PK. Anterior sclera undergoes thinning with increasing degree of myopia. *Invest Ophthalmol Vis Sci*. 2020;61:6.
22. Girard MJA, Strouthidis NG, Ethier CR, Mari JM. Shadow removal and contrast enhancement in optical coherence tomography images of the human optic nerve head. *Invest Ophthalmol Vis Sci*. 2011;52:7738−7748.